A Study Toward Energy Saving in Brick Making: Part 2 - Simulation Of Processes in Brick Kiln

S. Prasertsan, G. Prateepchaikul, T. Theppaya and P. Kirirat
Department of Mechanical Engineering
Prince of Songkla University
Hat Yai, Thailand 90110

ABSTRACT

Brick making in developing countries is a major firewood consumer. In the light of firewood shortage, there is a pressing need to develop an energy-efficient brick kiln suitable for rural production. A four-chamber batch-type downdraft kiln possessing heat recovery feature is proposed to substitute the conventional updraft kiln. In order to warrant the success of the proposed kiln, the whole system is studied by computer simulation. The system consists of cooling, firing, preheating and drying processes which simultaneously occur in the four chambers. The simulation covers the four processes in series and involves heat transfer, mass transfer and combustion of firewood. It was found that brick produced by this system consumes about 1200 kJ/kg brick which is substantially lower than that produced by the conventional updraft kiln while the production rate is increased 2.5 times

1. INTRODUCTION

In part 1 of this study, a general guideline for the reduction of fuel consumption in brick firing was given [1]. The study suggested that the energy requirement can be minimized by manipulating the firing temperature and time. It also recommended that the kiln should be small and the brick should be set in the manner to attain uniform temperature distribution in the kiln. Waste heat recovery should be incorporated in the kiln operation. All these suggestions are, in fact, the principle of the tunnel kilns which are widely used in large brick making factories. The operation of the tunnel kiln is a continuous process consisting of four simultaneous activities namely; drying, preheating, firing and cooling. However, the tunnel kiln is not suitable for the rural areas of developing countries because the capital cost is very high and the production rate is too high for local consumption. In developing countries, brick is produced and consumed locally because brick is a relatively cheap commodity which cannot afford high transportation cost. In addition, there is a seasonal variation in the demand of bricks. Construction works drastically increase in the dry season when labor forces from the agricultural sector are available. The kiln must also be designed to accommodate the fluctuation of demand. The batch firing kiln seems to be an appropriate technology. A moderate energy-efficient process is found in the snake kiln. The snake kiln is a moving fire tunnel kiln normally found in the earthen ware production. It is a batch type operation with partial heat recovery features. However, the loading and unloading of the ware is rather difficult and the batch cycle is long.

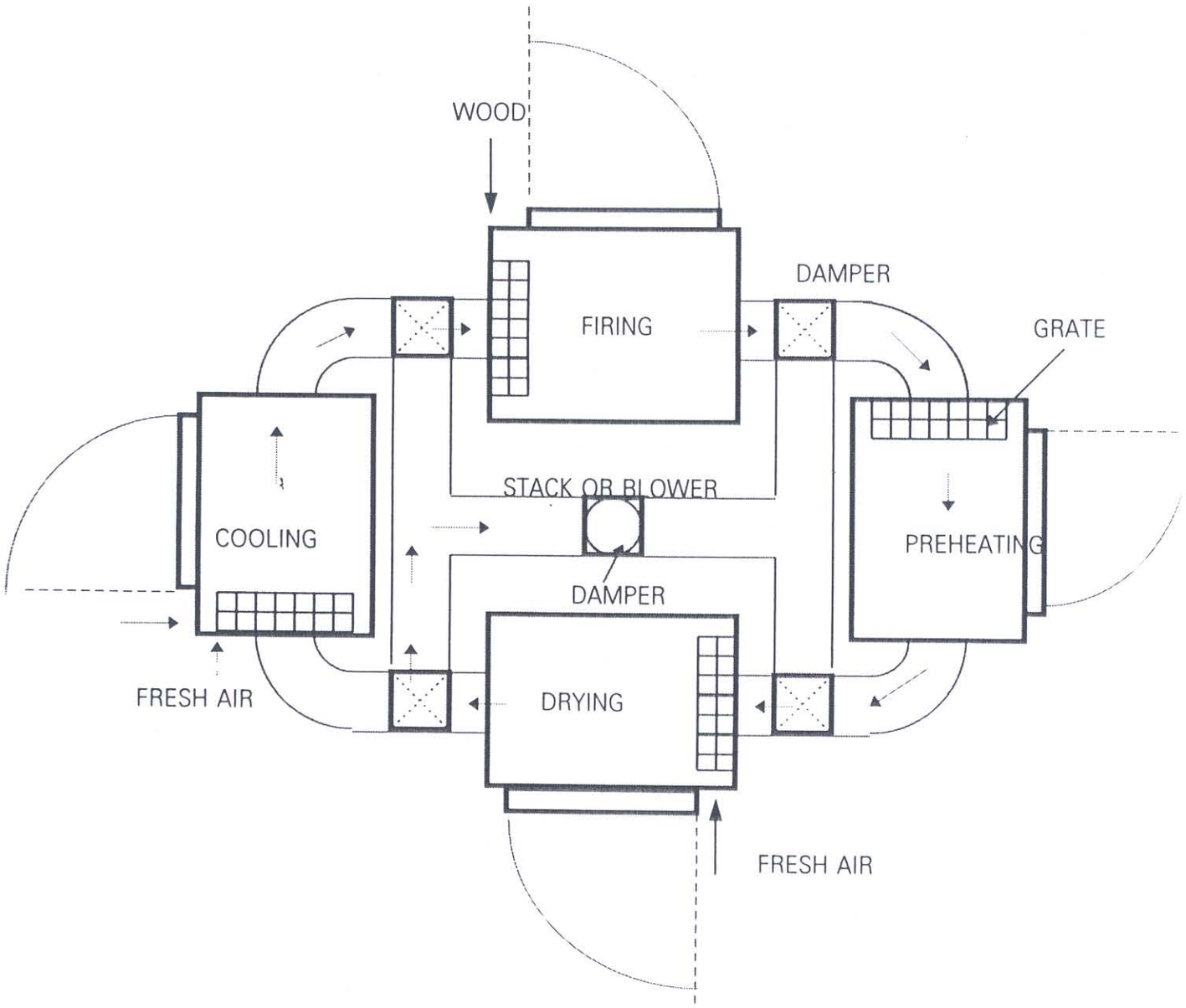

Fig. 1. Batch type continuous kiln.

Because the energy-efficient batch operation is the basic requirement of the brick making industry in developing countries, the kiln should incorporate the continuous process and heat recovery feature of the tunnel kiln to the batch-type kiln. This results in the kiln as proposed in Fig.1. The system consists of four downdraft kilns. Each kiln takes its turn to serve the four functions of the continuous kiln (drying, preheating, firing and cooling). The four kilns are connected by ducts which convey fresh air for cooling and hot gas for preheating and drying of the brick. This system can be the stand-alone (four) downdraft batch-type kilns or cooperative continuous kiln to serve the fluctuation of the brick market. The system is not wholely continuous and the batch characteristic of each chamber introduces the transient behavior to the process. Additional difficulties resulting from the requirement of time matching of the four different processes in the four chambers are expected. Therefore, the success of this system is still doubtful unless extensive analysis and verifying experiment are thoroughly studied. It is essential, therefore, to present the analysis of the system operation by computer simulation, which is the content of this paper. Verifying experiments are in progress and will be reported in due course.

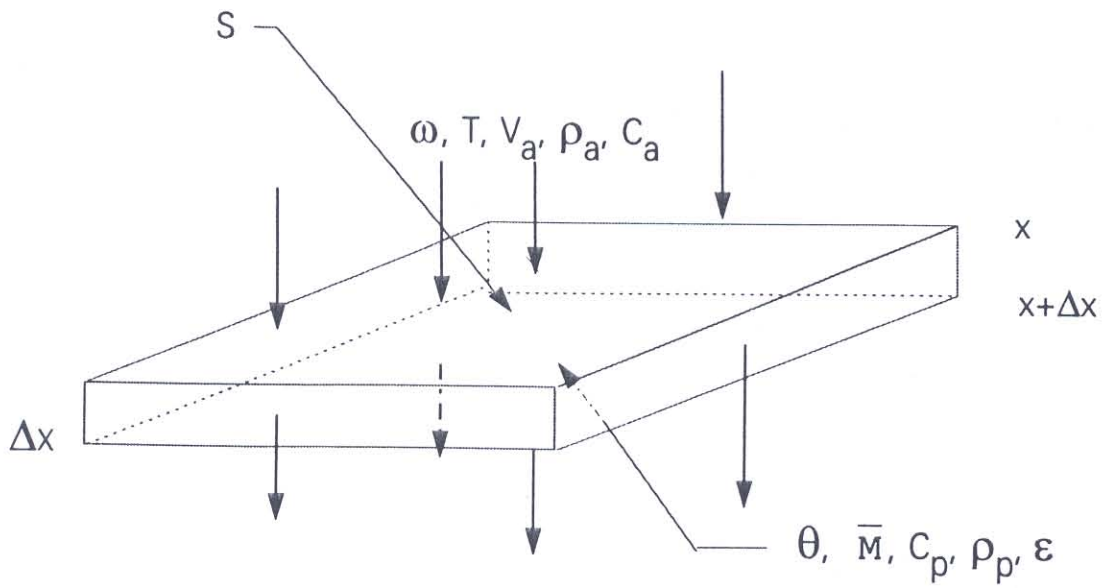

Fig. 2. Element of fixed bed model.

2. SIMULATION EQUATIONS

Heat transfer and mass transfer in each chamber are determined from the fixed-bed model. The brick pile is divided horizontally into elements of Δx thickness (Fig. 2). In each element, four equations are established based on heat and mass balance to determine the air temperature (T), brick temperature (θ), humidity of the air (ω) and average moisture content in brick ($\overline{M}$).

2.1 Air Temperature

Air temperature is examined from the change of enthalpies of the air flowing through the element and of the air in the void within the control volume Sdx. In the time interval dt, the change of enthalpy of the flowing air is,

$$\left(\rho_a V_a C_a + \rho_a V_a \omega C_v\right) \frac{\partial T}{\partial t} S dx dt \tag{1}$$

where ρ_a is air density, V_a is air velocity, C_a and C_v are heat capacity of air and water vapor, respectively. Sensible heat of air in the void is given by,

$$\left(\rho_a C_a + \rho_a \omega C_v\right) \frac{\partial T}{\partial t} S \varepsilon dx dt \tag{2}$$

where ε refers to the void ratio of the bed.

Convective heat transfer to the brick is,

$$q = ha\left(T-\theta\right) Sdxdt \tag{3}$$

where h is the convective heat transfer coefficient and a is the surface to volume ratio of the brick. The convective heat transfer coefficient is determined by

$$h = \frac{k_a}{D_p} Nu$$

where k_a is the conduction heat transfer coefficient of the air, D_p is the characteristic length of the brick and Nu is the Nusselt number.

$$Nu = c(Re)^n$$

For $2500<Re<8000$; $c=0.160$, $n=0.699$
$8000<Re<100\,000$; $c=0.092$, $n=0.675$

where Re is Reynold's number.

Equate equations (1), (2) and (3) and rearrange to obtain,

$$V_a\frac{\partial T}{\partial x} + \varepsilon\frac{\partial T}{\partial t} = \frac{-ha}{\rho_a C_a + \rho_a \omega C_v}\left(T-\theta\right) \tag{4}$$

2.2 Brick Temperature

Heat transferred to the brick causes the evaporation of moisture (sensible and latent heat) and sensibly heats up the brick. The change of enthalpy of the brick in the time interval dt is,

$$\left(\rho_p C_p + \rho_p C_w \overline{M}\right)\frac{\partial \theta}{\partial t} Sdxdt \tag{5}$$

where C_w is the heat capacity of water.

Moisture removed from the brick is given by,

$$G_a\frac{\partial \omega}{\partial x} Sdxdt \tag{6}$$

where G_a represents the mass flux velocity and given by,

$$G_a = V_a \rho_a$$

Thus, enthalpy associated with the moisture removal is,

$$h_{fg} G_a \frac{\partial \omega}{\partial x} S dx dt + C_v G_a (T-\theta) \frac{\partial \omega}{\partial x} S dx dt \tag{7}$$

where h_{fg} is the latent heat of water.

Equate equations (3), (5) and (7) to get,

$$\frac{\partial \theta}{\partial t} = \frac{ha}{\rho_p C_p + \rho_p C_w \overline{M}} (T-\theta) - \frac{h_{fg} + C_v (T-\theta)}{\rho_p C_p + \rho_p C_w \overline{M}} G_a \frac{\partial w}{\partial x} \tag{8}$$

2.3 Humidity of Air

Humidity of the air flowing through the bed is determined from the mass of moisture removed from the brick. The change of air humidity in the interval dt is,

$$G_a \frac{\partial \omega}{\partial x} S dx dt + \varepsilon \rho_a \frac{\partial \omega}{\partial t} S dx dt \tag{9}$$

Meanwhile, the change of moisture in the brick is given by,

$$\rho_p \frac{\partial \overline{M}}{\partial t} S dx dt \tag{10}$$

The conservation of mass, Eq. 11, is obtained by equating expressions (9) and (10) and by neglecting the term $\partial\omega/\partial t$ because it is very small compared to $\partial\omega/\partial x$,

$$\frac{\partial \omega}{\partial x} = \frac{\rho_p}{G_a} \frac{\partial \overline{M}}{\partial t} \tag{11}$$

2.4 Moisture of Brick

The brick moisture is obtained from the thin-layer drying equations. The empirical equations for drying clay product are [2],

For V_a<100 cm/s,

$$\frac{\partial \overline{M}}{\partial t} = \frac{4.3 \times 10^{-10}}{m_b} L^{0.73} B^{0.8} (P_s - P_v)(1 + 0.121 V_a^{0.85}) \tag{12}$$

For 100<V_a<300 cm/s,

$$\frac{\partial \overline{M}}{\partial t} = \frac{2.12 \times 10^{-10}}{m_b} L^{0.77} B (P_s - P_v)(1 + 0.121 V_a^{0.85}) \tag{13}$$

where m_b is the mass of brick, L is the length of the brick in the direction parallel to the flow, B is the breadth of brick while P_s and P_v are the saturated pressure and vapor pressure, respectively.

Equations (4), (8), (11) and (12) or (13) are used in the simulation to determine the temperatures of the air and the brick and the associated humidity or moisture. In the simulation, the pile of brick has a dimension of 2.1x2.1x1.6 m^3 and is divided into 24 sections. The simulation requires the conditions (T, ω) of the hot gas which have to be computed from the combustion equation of the firewood.

2.5 Combustion of Firewood

Firewood in this study is rubber wood. Ultimate analysis of rubber wood found that the wood can be represented chemically by $C_{3.841}N_{0.0136}H_{5.65}O_{2.805}$ and 4% ash [3].

The combustion equation is, therefore, written as,

$$C_{3.841}N_{0.0136}H_{5.62}O_{2.805} + 3.8435\,(Y)\,(O_2 + 3.76N_2) + (n_{H_2O})H_2O \rightarrow$$
$$3.841CO_2 + (2.81 + n_{H_2O})H_2O + 3.8435\,(Y-1)O_2 + (14.452Y + 0.0068)N_2 \tag{14}$$

where Y is the fraction of theoretical air.

The number of mole of water in the combustion air, n_{H2O}, is obtained from

$$n_{H_2O} = \left[\frac{\omega_a (3.8435Y(1+3.76))M_a}{M_{H_2O}}\right] \tag{15}$$

where M_a and M_{H2O} are the molecular weight of air and water, respectively.

Firewood consumption rate is derived from equation (14) as,

$$\dot{m}_f = \frac{\dot{m}_a}{\left[3.8435Y(1+3.76)\frac{M_a}{M_f}\right]} \tag{16}$$

where M_f is the molecular weight of fuel while $\dot{m}_f$ and $\dot{m}_a$ are mass flow rate of fuel and air, respectively.

Taking the combustion chamber as the controlled volume, the reactants entering the controlled volume are air and firewood. The combustion product leaving the controlled volume is treated as mixture of ideal gases which the specific heat at a particular temperature is determined from the mole fractions of the product components. Mole fractions of product components are obtained from equation (14). The combustion temperature is determined from the enthalpy of the product assuming an adiabatic controlled volume.

$$h_c = \left[\frac{m_f \omega_f h_w + \dot{m}_f HV + \dot{m}_a h_a + \dot{m}_a \omega_a h_{ga}}{\dot{m}_c} \right] \tag{17}$$

where HV is the heating value of fuel. Alternatively h_c can be represented by,

$$h_c = C_c T_c \tag{18}$$

where C_c is a function of temperature and the mole fraction of product components and $\dot{m}_c = (1+\omega_a)\dot{m}_a + 0.96\ \dot{m}_f$. Enthalpies in equations (17) and (18) are referenced at 0°C. The combustion temperature and the associated air flow rate for one firewood consumption rate are derived from equations (14)-(18).

In the actual operation the combustion air is the air preheated by the (brick) cooling process when its temperature decreases with time. That is, h_a in equation (17) steadily decreases during the firing. Thus, if the firing temperature is kept constant, the air flow rate and/or firewood consumption rate must be altered. If the air flow rate is not changed, more wood is required. Alternatively, if wood consumption rate is not altered, less air must be allowed. It is likely that the latter is preferable since wood can be saved. However, the decreasing air flow rate will affect the upstream processes (preheating and drying). In conclusion, the nature of batch operation introduces the transient behavior in the simulation.

3. SIMULATION OF THE PROCESSES

In the simulation of the cooling, firing and preheating chambers, where only heat transfer occurs, the air and brick temperatures at each layer are determined by equations (4) and (8). The moisture content in the brick in the preheating chamber is very low and is assumed of having no effect on the simulation. Heat and mass transfer characteristics in the drying chamber are obtained by solving equations (4), (8), (11) and (12) or (13). The sequence of simulation is illustrated in Fig.3. Fresh air is drawn into the cooling chamber at a constant mass flow rate. The air flow rates used in the simulation are 600 kg/h, 800 kg/h, 1000 kg/h, 1200 kg/h, 1400 kg/h and 1600 kg/h. The working air in the firing chamber and beyond takes into account the mass of the burnt firewood. Additional fresh air is introduced into the drying chamber to adjust the air temperature constant at 150°C, which is considered suitable for the process. The kiln capacity in the simulation is about 4,700 bricks per chamber. Each brick has the dimension of 19.0x8.0x6.5 cm^3 and four rectangular holes in axis direction. The hole dimension is 1.5x1.5 cm^2. Unit weight is 1.5 kg/brick. The initial moisture content in the green brick in the drying chamber is 12% dry basis. The end of each cycle is defined by the condition that the

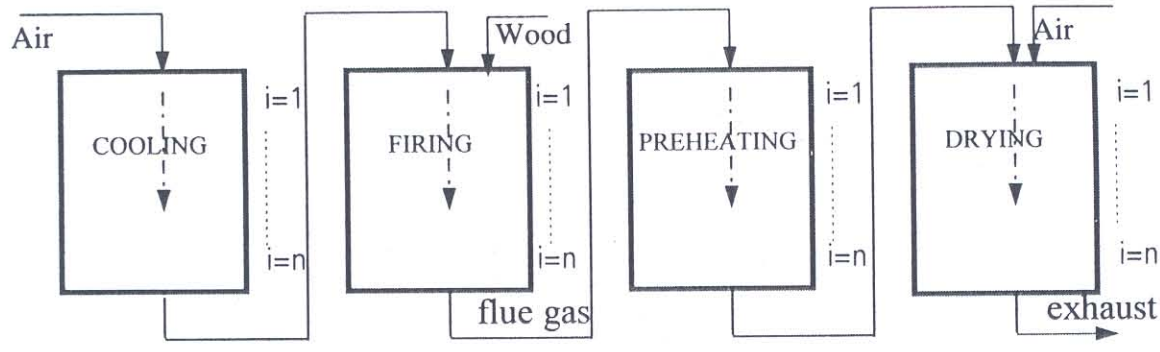

(a)

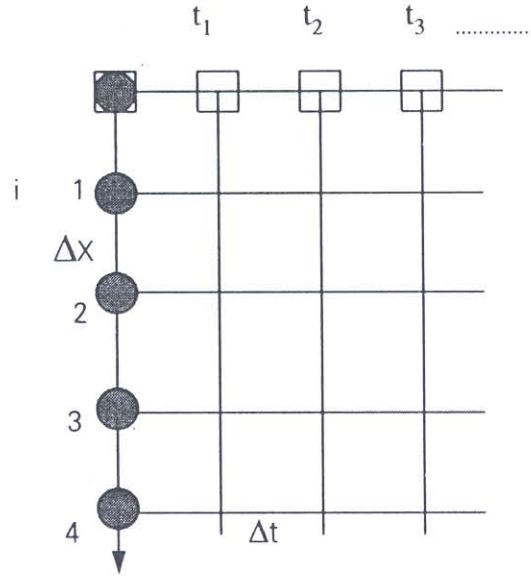

1) Set initial and boundary condition

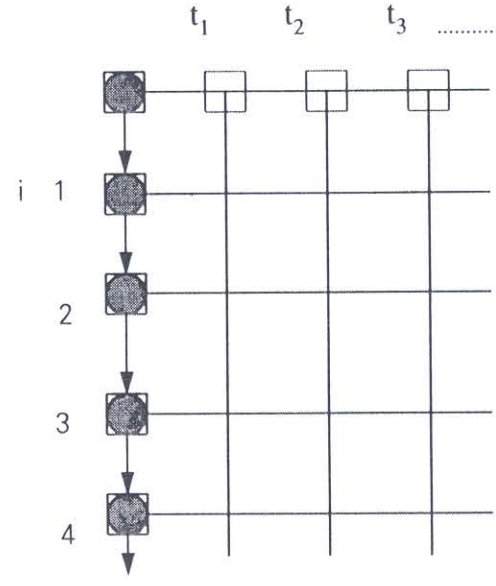

2) Compute state of air at each layer

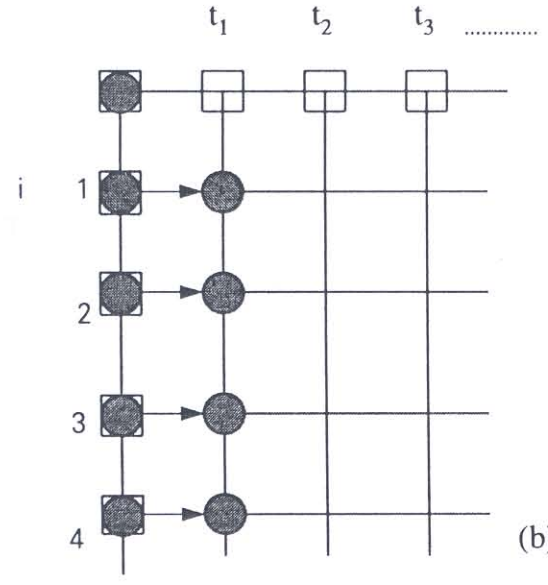

3) Compute state of brick at time t_1

(b)

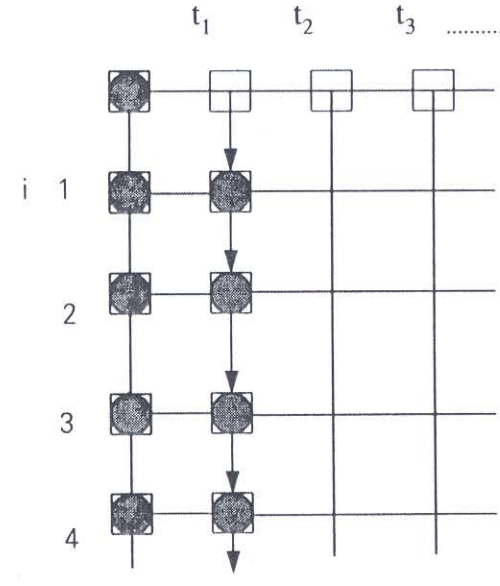

4) Compute state of air at each layer at time t_1

Fig. 3. Physical model of simulation (a) Train of four chambers (b) Simulation sequence in each chamber, θ and $\overline{M}$ are represented by ●; T and ω are represented by ❑

temperature of the brick at the bottommost layer of the firing chamber reaches 650°C. The clay-to-brick transformation temperature is 600°C [1]. Three firing temperatures 700°C, 800°C and 900°C are simulated.

The simulation starts by setting initial temperatures of the brick at the uppermost and bottommost layers. For example, in the cooling chamber the corresponding temperatures of the two layers are equal to the firing temperature and 650°C. A similar temperature distribution profile is initially assumed for the firing and preheating chambers. The initial temperature of the drying chamber is 30°C. Iteration procedure of the simulation keep checking the convergence and the continuity of the temperature of all chambers. The convergence tolerance of the iteration is 5°C.

4. RESULTS AND DISCUSSION

Fig. 4 gives the (preheated) combustion air temperature and wood consumption rate during the firing process. The conditions for the simulation are; fixed air flow rate of 1000 kg/h and flame temperature of 800 °C. The combustion air is heated up in the brick cooling chamber. Because the brick temperature decreases with time, the combustion air temperature decreases from 165°C to 133°C during the firing time of 522 minutes. As the combustion air temperature is decreasing, the firewood consumption rate gradually increases from 52.5 kg/h to 57.1 kg/h in order to maintain the flame temperature at 800°C. Alternatively, the flame temperature and wood consumption rate can be kept constant by reducing the air flow rate during the course of firing. However, in actual practice, the kiln operator prefers to control the firing temperature by controlling the wood consumption rate rather than

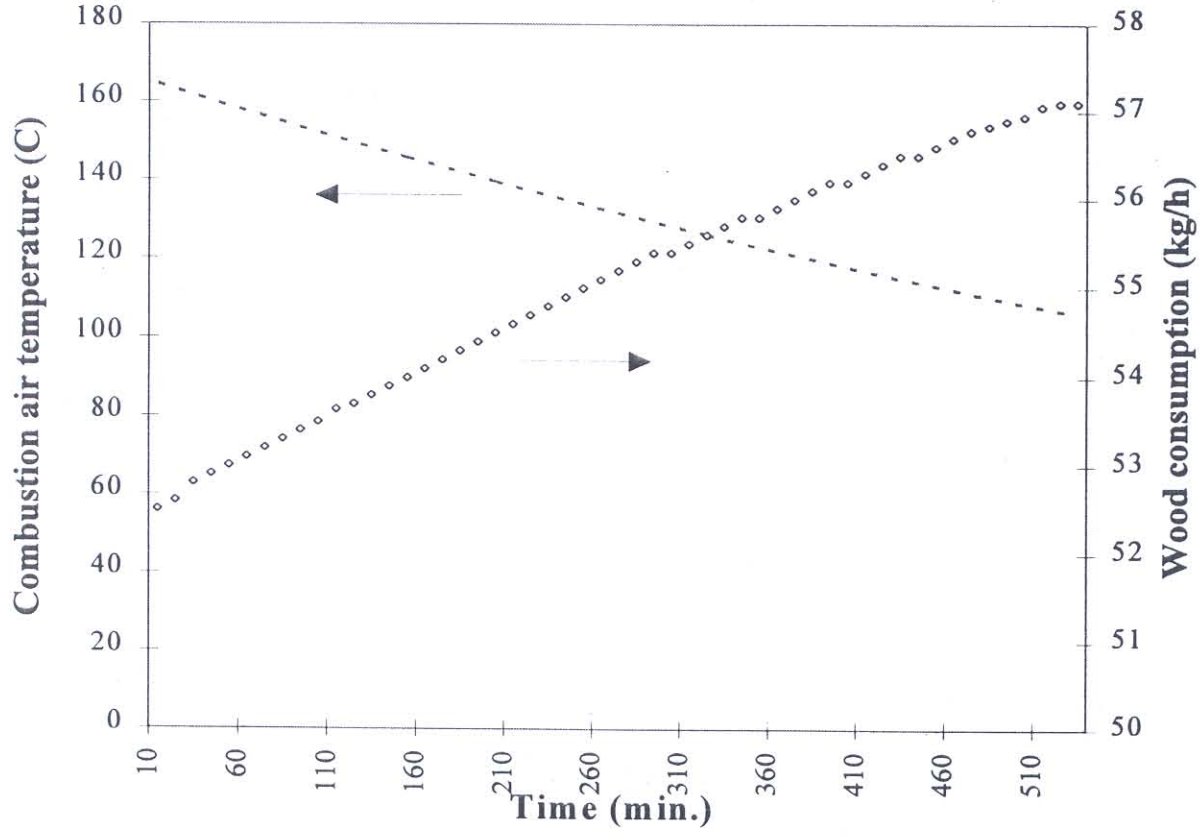

Fig. 4. Temperature of combustion air wood consumption rate (Flame temperature 800°C, cooling air flow rate 1000 kg/h).

the air flow rate. Because the wood consumption rate increases only 4.6 kg/h for the whole course of firing (about 8.5 hours), it is more practical to say that the furnace attendant should be instructed to burn the wood at the constant rate of 55 kg/h. Total wood consumption is 480 kg. Similar to the firing chamber, the air temperature in the drying chamber is constant, but at 150°C. Because the air leaving the preheating chamber (entering the drying chamber) increases its temperature with time, more fresh air must be drawn into the drying chamber as the time elapses, Fig.5. In the operation, the fresh air flow rate of 3,200 kg/h at the beginning of the cycle must be adjusted to 3,850 kg/h at the end of the cycle.

Temperatures of the bricks at the bottommost layers of the four chambers and the corresponding air temperatures, which vary with time, are shown in Fig.6. The temperature of the bricks (bottommost layer) in the cooling chamber which is 650°C at the beginning of the cycle is cooled down to 420°C. The working air leaving the cooling chamber has a temperature of 180°C and 105°C at the beginning and the end of the cycle, respectively. This air temperature is relatively low in comparison to the brick because of its high mass flow rate (1000 kg/h). The final temperature of the brick (420 °C) is also very high. A lower temperature is achievable by extending the processing time. However, the cycle duration is determined by the firing process and lengthening the firing time is undesirable in terms of energy. Alternatively, the end of the process can be defined by the brick temperature at the bottom of the cooling chamber. After the bottommost bricks in the firing chamber reach 650°C, the firing process is ceased but the cooling process is still going on until its temperature reaches, say, 80°C. This will inevitably extend the cycle time but, consequently, will shorten the successive cycle time because the initial temperature in the cooling chamber (in the next cycle) will be less. The cycle time will be alternately long and short.

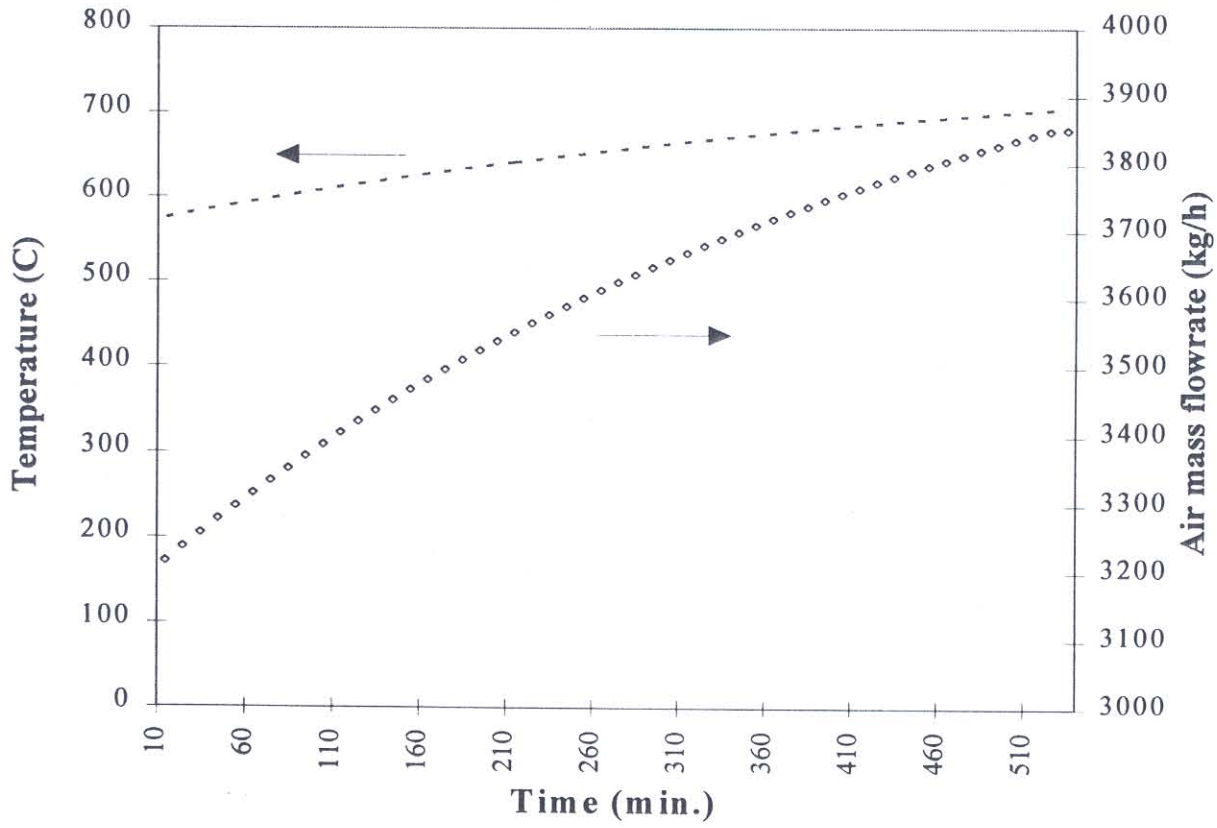

Fig. 5. Temperature of preheating chamber outlet and flow rate of fresh air inlet at drying chamber (Flame temperature 800°C, cooling air flow rate 1000 kg/h).

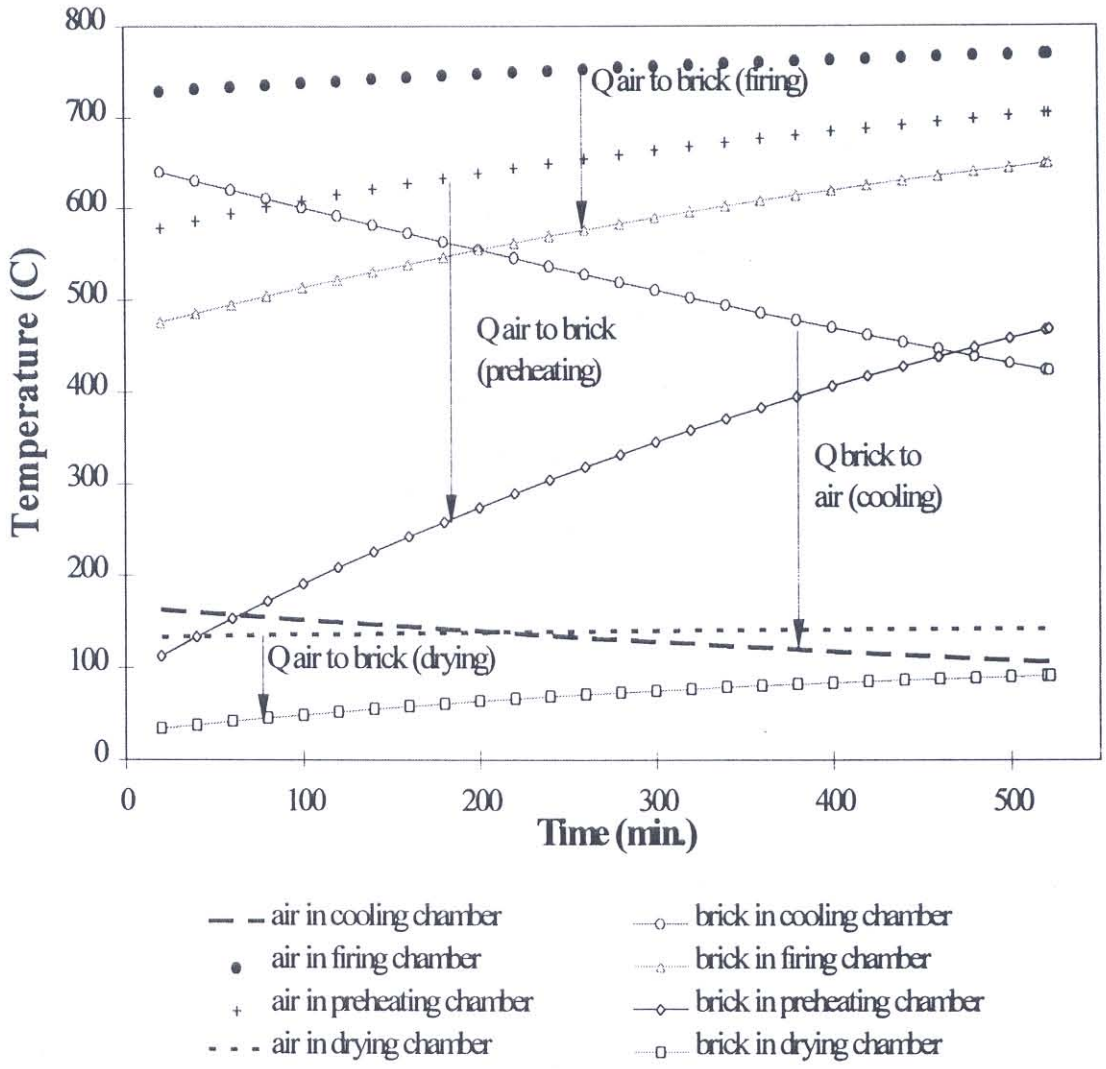

Fig. 6. Changes of bottommost brick temperature and outlet air temperature of the four chambers (Flame temperature 800°C, cooling air flow rate 1000 kg/h).

The temperature of the bottommost bricks in the firing chamber increases from 475°C to 650°C during the course of the firing, an increase of 175°C. Although the flame temperature is constant at 800°C, the temperature of the gas leaving the firing chamber is 725°C at the start of the cycle and increases to 775°C at the end. In the preheating chamber, the brick is heated up from the initial temperature of 100°C to 475°C while the corresponding temperatures of the working air are 580°C and 700°C. The temperature of the air entering the drying chamber is constant at 150°C which results in a brick temperature of 100°C in the drying chamber.

The above discussion is limited to the states of air and brick at the bottom of the four chambers only. In the downdraft process one can expect higher temperature at the top layer. The temperature distribution along the depth of the brick pile at the end of the cycle is shown in Fig.7. It is clear that the temperature differences of the top and the bottom bricks in all chambers are less than 100°C and no significant temperature difference occurred in the drying chamber. The change of brick moisture with respect to time and depth of bed is presented in Fig.8. The moisture content of the brick decreases linearly with time. At the end of the cycle, the moisture content of the top layer and bottom layer bricks are 7.6% and 8.7%, respectively.

The discussion so far is based on one operating condition only (flame temperature 800°C and cooling air flow rate 1000 kg/h). However, similar behavior can be envisaged for other conditions with

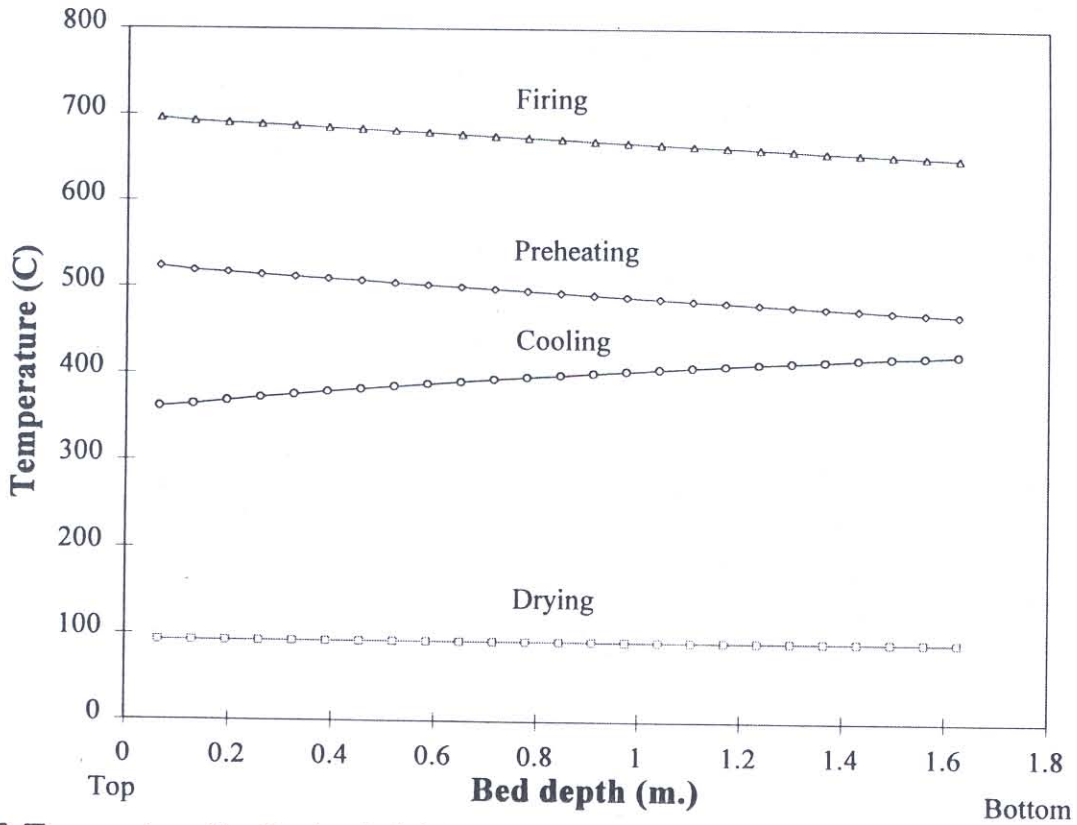

Fig. 7. Temperature distribution in brick pile at the end of cycle (Flame temperature 800°C, cooling air flow rate 1000 kg/h).

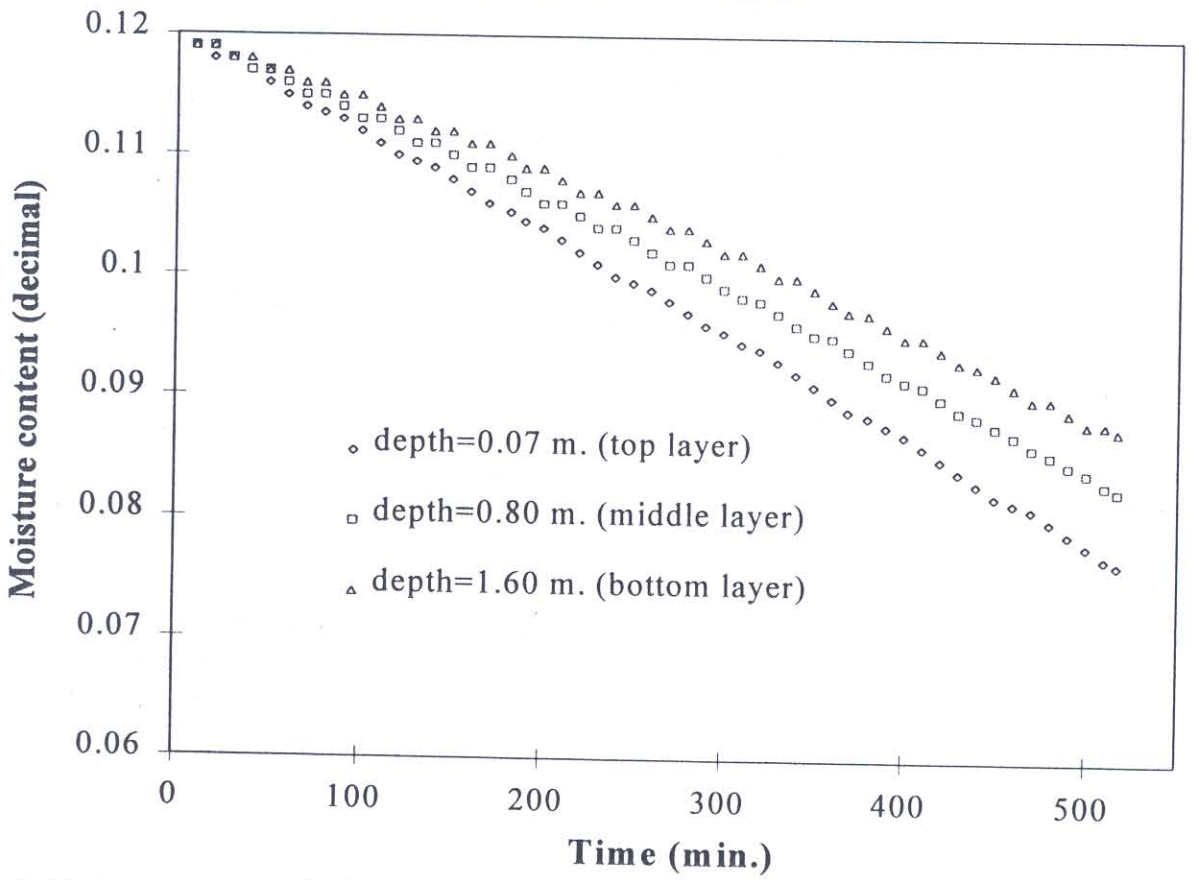

Fig. 8. Moisture content of brick in drying chamber (Flame temperature 800°C, cooling air flow rate 1000 kg/h).

a certain degree of (quantitatively) different results. For example, the trends of brick moisture in the drying chamber for 700°C and 900 °C flame temperatures are similar to that of 800 °C. That is, the difference in moisture content of the top and bottom layers is approximately 1%. However, the operations with 700°C and 900°C flame temperatures give the final moisture contents of the top layer bricks of 5.2% and 8.5%, respectively, because the brick fired at 700°C flame temperature needs 852 minutes to finish which is 467 minutes longer than that fired at 900°C. Since drying temperature is 150°C for every firing temperature, the operation with longer cycle time (700°C) will result in a lower moisture content.

Wood consumption varies with the flame temperature and combustion air flow rate as presented in Fig.9. In order to maintain a constant flame temperature, the higher air flow rate requires more wood, although the firing time is shorter. Brick fired at lower temperature takes a longer firing time; which results in a higher wood consumption. The roles of the firing temperature and cooling air flow rate on the energy and firing time are shown in Table 1. It is obvious that for a particular firing temperature, the operation for minimum energy is achieved at the expense of a longer firing time (lower production rate). At every firing temperature, firing with an air flow rate of 1600 kg/h consumes 35% more wood (and specific energy) than that of 600 kg/h flow rate while the firing time is halved. Furthermore, firing at lower temperature consumes more wood and takes a longer time. It is, therefore, recommended that the brick should be fired at high temperature if energy cost is critical.

The specific energy consumption in this simulation is different from those reported in Prasertsan and Theppaya [1] because the figures are referenced to different temperatures. For example, brick fired at 800°C in this simulation leaves the system at a temperature of about 400°C but the experiment in [1]

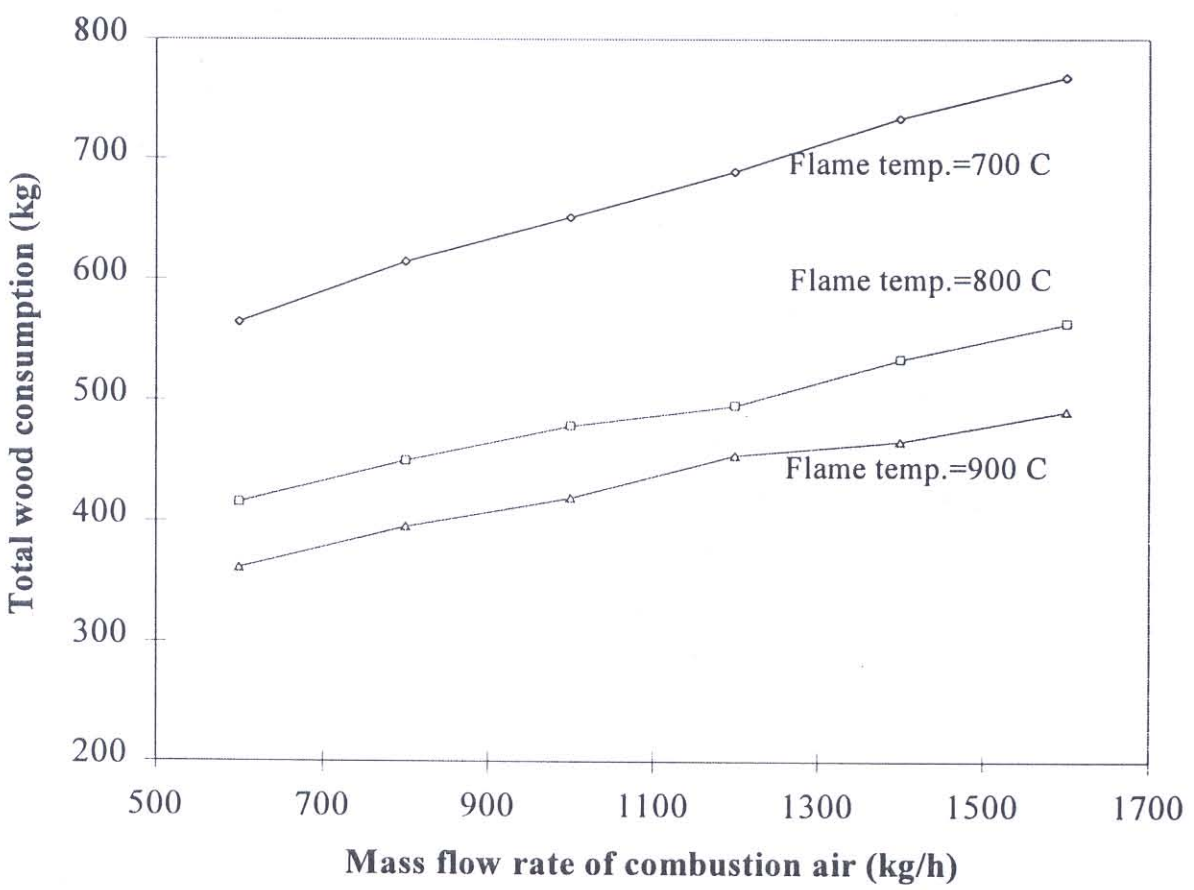

Fig. 9. Total wood consumption of different operating conditions.

Table 1. Simulation results.

Flame temperature (°C)	Mass flow rate of combustion air (kg/h)	Total wood consumption (kg)	Average wood consumption rate (kg/h)	Specific energy (kJ/kg brick)	Firing time (min.)	Rate of energy input (kW)
700	600	564.4	26.9	1379.8	1260	129
	800	614.5	36.3	1502.3	1015	174
	1000	651.2	45.9	1592.0	852	220
	1200	689.6	55.4	1685.8	747	265
	1400	734.0	66.0	1794.4	667	316
	1600	768.4	74.7	1878.4	617	358
800	600	415.8	32.2	1016.5	774	154
	800	450.2	43.6	1100.6	620	209
	1000	478.9	55.0	1170.8	522	264
	1200	495.7	66.5	1211.7	447	319
	1400	533.6	78.1	1304.3	410	374
	1600	563.3	89.6	1377.1	377	429
900	600	361.8	38.4	884.4	566	184
	800	395.9	51.9	967.8	458	248
	1000	419.6	65.4	1025.7	385	313
	1200	454.7	79.1	1111.5	345	379
	1400	466.3	92.6	1139.0	302	443
	1600	491.2	106.4	1200.7	277	509

gave the specific energy at the firing temperature, i.e., 800°C. If the heat capacity of the brick is taken into account, the specific energy of the two studied are in the same range. However, it should be noted that in the simulation there are many assumptions which may, to a certain extent, differ the results from the actual practice. As the firing time is inversely proportional to the specific energy, it is, perhaps, appropriate to take the input power (kW) as an operating criterion. If this is the case, it is likely that the firing temperature and air flow rate should be low (Table1).

The rate of firewood consumption depends on the temperature of the combustion air and percentage of theoretical air. The two parameters give the flame temperature in the firing chamber. Therefore, if the temperature in the firing chamber is fixed, the firewood consumption rate is controlled by the flow rate of the combustion air. In this simulation, the firing process ends only when the temperature of every brick reaches at least 650°C. Furthermore, if the air flow rate is very low (due to a low wood consumption rate), the cooling and drying of brick may not be effectively achievable. If the air flow rate is high, the processing time is shortened but the specific energy could be high due to a high brick outlet temperature. The appropriate operation is, therefore, a matter of time and energy matching management of the four chambers.

5. CONCLUSION

In an attempt to understand the batch-type brick kiln with heat recovery features, the four processes namely; cooling, firing, preheating and drying were studied by computer simulation. The role of combustion air flow rate and firing temperature were thoroughly studied. It was concluded that the brick should be fired at a high temperature so that less energy is required and a high production rate is obtained, unless the input power is the operating criterion. The designed kiln and process result in an energy-efficient brick firing method. The kiln can serve as four stand-alone downdraft kilns or cooperative continuous kiln to meet the market demand. It is believed that the system is suitable for the brick industry in most developing countries.

6. ACKNOWLEDGMENT

This work was carried out with financial support from the National Science and Technology Development Agency (Thailand).

7. NOMENCLATURES

a = surface to volume ratio of brick (m^{-1})
B = breadth of brick (cm)
C = heat capacity (kJ/kg °C)
D = characteristic length (m)
G = mass flux velocity (kg/m² s)
h = convective heat transfer coefficient (W/m °C), specific enthalpy (kJ/kg)
k = conduction heat transfer coefficient (W/m °C)
L = length of brick in the direction parallel to the flow (cm)
m = mass (g)
M = molecular weight
Nu = Nusselt number
P = pressure (mm. Hg)
q = heat (kJ)
Re = Reynold's number
S = bed crossectional area (m²)
t = time (s)
T = air temperature (°C or K)
V = velocity (m/s, otherwise stated)
x = bed thickness (m)
Y = fraction of theoretical air (decimal)

ρ = density (kg/m³)
ω = air humidity ratio (decimal)
θ = average brick temperature (°C)
ε = void ratio (decimal)
$\overline{M}$ = brick moisture (decimal)

Subscripts

a = air
b,p = brick
c = combustion product
f = fuel
s = saturation condition
v = water vapor
w = water

8. REFERENCES

1. Prasertsan, S. and Theppaya, T. (1995), A study toward energy saving in brick making: Part 1 - Key parmeters for energy saving, *RERIC International Energy Journal*, 17(2): 143-154.
2. Singer F., and Singer, S.S. (1963) *Industrial Ceramics*, Chapman & London.
3. Prasertsan, S. (1993), Energy Value of Rubber Plantation Residues, *R&D J. Eng. Inst. Thailand*, 4(2): 13-22.